Research on a controlled high voltage power supply for Power Processing Unit

IEPC-2019-937

Presented at the 36th International Electric Propulsion Conference
University of Vienna • Vienna, Austria
September 15-20, 2019

Qing Kang,[1] Xuan Zhang, Jie Xing and Feng Li
China Academic of Space Technology, Beijing, 100094, China

and

Lie Xu[2], Ran Liu
Tsinghua University, Beijing, 100084, China

Abstract: With the development of power electronic device technology, the continuous advancement of wide band gap devices has promoted the development of space power supplies. This paper introduces a general-purpose high-voltage power module based on Dual Active Bridge(DAB) topology, carries out theoretical analysis, designs the control method, and establishes a simulation model based on Matlab / Simulink, which verifies that the proposed control strategy is feasible and effective. A solution for space electric propulsion high voltage power supply is provided.

Nomenclature

U_H = withstand voltage of the full-bridge converter DC bus capacitor
C_H = the capacitance of the full-bridge converter DC bus capacitor
I_H = the full-bridge converter device current stress
P_{SW} = the switching loss of the single-switch converter of the full-bridge converter
P_{SS} = the on-state loss of a single switching device for a full-bridge converter
U_{dc1} = primary DC voltage
U_{dc2} = secondary DC voltage

I. Introduction

ELECTRIC Propulsion (EP) is gradually being used for orbital raising (OR) and station keeping (SK) in commercial communications satellites, deep space exploration. Currently, there are several EP: Hall Effect Thruster (HET), Gridded Ion Engine (GIE) technology and High Efficiency Multistage Plasma (HEMP) [1]. The generic building blocks for beam supply in PPU for GIE and the anode supply in PPU for HET are high voltage power supply (HVPS) module [2-7].Traditionally, uncontrolled rectification is applied in HVPS. However, synchronous rectification is enabled gradually thanks to the development of SiC and GaN components, which is helpful to increase the efficiency [8].

[1] Senior Engineer, Institute of Telecommunication Satellite, jenny1115@163.com.
[2]Associate Professor, Department of Electrical Engineering, xulie@mail.tsinghua.edu.cn .

II. Theory of Operation

A. Topology design

The DC-DC converter topology using HFT isolation can be considered to consist of two parts, the primary side and the secondary side. The primary side is a DC/AC inverter and the secondary side is an AC/DC rectifier. At present, limited by the capability of the aerospace-class components, the secondary side of the high-voltage power supply in the PPU adopts uncontrolled rectification scheme with diodes. With the development of wide gap components as SiC or GaN, synchronous rectification can be realized gradually in space. Therefore, the topology of the controllable MOSFET is analyzed and compared on the secondary side. The DC/AC inverter and the AC/DC converter have three configurations of a full bridge structure, a half bridge structure, and an asymmetric half bridge, respectively.

Table 1 compares the number of components required, the DC capacitor parameters, current, and losses of the full-bridge, half-bridge, and asymmetric half-bridges under the same power and the same DC voltage. U_H is the withstand voltage of the full-bridge converter DC bus capacitor, C_H is the capacitance of the full-bridge converter DC bus capacitor, I_H is the full-bridge converter device current stress, and P_{SW} is the switching loss of the single-switch converter of the full-bridge converter, P_{SS} is the on-state loss of a single switching device for a full-bridge converter.

Table1. Comparison for full bridge, half bridge and asynchronous half-bridge topology

	Full bridge	Half bridge	Asynchronous half-bridge
Number of components	4	2	2
Capacitance	$(U_H, C_H)\times1$	$(0.5U_H, >2C_H)\times2$	$(U_H, C_H)\times1$
DC current	I_H	I_H	I_H
AC current	I_H	$2I_H$	$2I_H$
Switching loss	$4P_{SW}$	$2\times2P_{SW}$	$2\times2P_{SW}$
On-state loss	$4P_{SS}$	$>4P_{SS}$	$>4P_{SS}$
Performance	high	low（Voltage fluctuation）	low（DC bias）

The power required for the electric propulsion power source is large, so the full-bridge converter is selected as the inverter structure of the high-frequency inverter and the high-frequency rectifier. Inverter and rectifier converters using a full-bridge converter as a high-frequency isolated DC-DC converter can be classified into a high-frequency resonant network and a high-frequency resonant network.

Since the secondary side of the LCC converter is a current source type port, it is necessary to ensure a current path, which is not as flexible as the LLC converter. Moreover, it has a large DC inductance on the secondary side, which affects the system power density. The current value of the dual voltage source port LLC converter is higher than that of the DAB converter, and the secondary side is ZCS. However, its modulation mode changes the switching frequency, which makes the control and filtering difficult, and the resonant frequency is greatly affected by the parameters. It is difficult to achieve parallel current sharing with respect to the DAB converter. So the DAB topology is applied in this paper.

B. Control method

For a DAB converter, the primary and secondary DC voltages are U_{dc1} and U_{dc2}, respectively, and the primary and secondary AC voltages are u_1 and u_2, respectively, as shown in Figure 1.

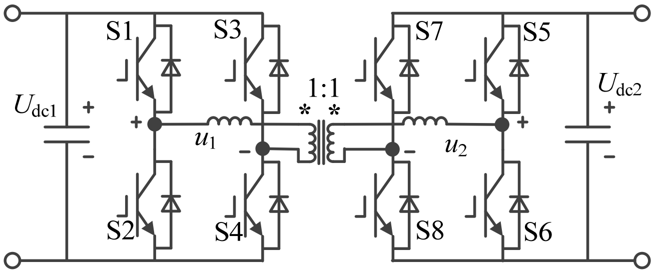

Figure 1. Circuit diagram of DAB converter

For the double-winding high-frequency transformer in the DAB converter, self-leakage inductance of the winding is set to be $L_{1,1\sigma}$, $L_{2,2\sigma}$, and the magnetizing inductance of the series structure is L_m, the self-inductance coefficient satisfies $L_{11}= L_{m+} L_{1,1\sigma}$, $L_{22}= L_{m+} L_{2,2\sigma}$ and the mutual inductance $M_{12}= L_m$. Set the excitation circuit current $i_m= i_{1+} i_2$ and the transformer back EMF as :

$$e = -L_m \frac{di_m}{dt}$$

Then there is:

$$\begin{bmatrix} u_1 - i_1 R_1 \\ u_2 - i_2 R_2 \end{bmatrix} + \begin{bmatrix} e \\ e \end{bmatrix} = \begin{bmatrix} L_{1,1\sigma} & 0 \\ 0 & L_{2,2\sigma} \end{bmatrix} \frac{\mathrm{d}}{\mathrm{d}t} \begin{bmatrix} i_1 \\ i_2 \end{bmatrix} \tag{1}$$

There are three control degrees of freedom for the DAB converter, which are the duty cycle of the primary secondary voltage waveform and the phase shift angle between the bridges. When General Phase-Shift Modulation (GPM) is used, the duty ratio and phase of the two H-bridges of the DAB converter can be arbitrarily set. The internal shift of the H-bridge can be defined as the phase shift angle between the two bridge arm drive signals within the H-bridge divided by π. Then the internal shift of the first H-bridge is compared to D_1=1-2d_1[0,1) (the duty ratio of the first H-bridge output is d_1), and the internal shift of the second H-bridge is compared to D_2=1-2d_2[0,1)（(the duty ratio of the second H-bridge output is d_2).

The shift in the sense of the bridge arm between the two H-bridges defining the two-port DAB converter is compared to D_0 being the phase shift angle between the reference bridge arms of the two H-bridges divided by π. The switching angular frequency is $\omega=2\pi f=2\pi/T$.

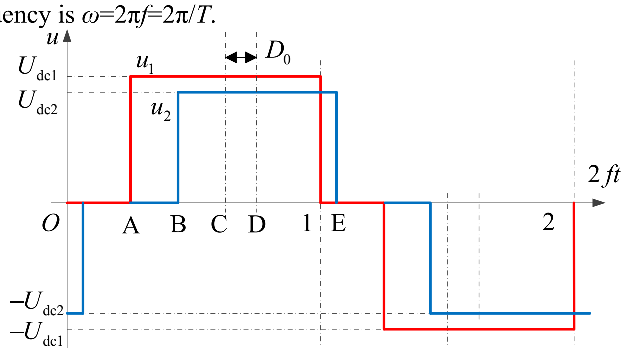

Figure 2. **Voltage waveforms of DAB**

When the DAB converter adopts the single phase-shift modulation (SPM) method, the duty ratio of the two square waves is always 50%, and the power transmission is controlled by adjusting the external phase shift angle D_0. The relationship between the inter-bridge phase shift phase angle D_0 and the system output power under the SPM method is:

$$P = \frac{nU_{dc1}U_{dc2}}{2fL} D_0 (1 - |D_0|) \tag{2}$$

Where n is the transformer ratio. The power characteristic of DAB is a quadratic function. For D_0, it is an odd function. When D_0>0, it is an even function with respect to D_0+0.5. The maximum value of power is obtained when D_0=0.5.

In the case of d=1, the expression of the current peak stress in the SPM method is $\frac{|D_0|U_{dc}}{2fL}$,which is proportional to $|D_0|$, and the current at the switching moment just reaches the peak value, and the ZVS soft switching characteristic can be guaranteed in the full power domain. At the same transmission power, there are two different out shift-phase angle cases with absolute values greater than 0.5 and less than 0.5. When the absolute value of the phase-shift phase angle is greater than 0.5, the system current stress is larger and the loss is larger. Therefore, the absolute value of the phase shift phase angle is less than 0.5, that is:

$$D_0 = sign(\mathrm{P})\frac{1}{2}[1-\sqrt{1-\frac{8fLP}{nU_{dc1}U_{dc2}}}] \tag{3}$$

In this case, the power has a monotonic relationship with the internal phase angle, and the system can be reliably controlled using a simple voltage PI closed-loop regulator.At steady state, the current on the DAB inductor under SPM modulation is a piecewise linear characteristic, as shown in Figure 3.

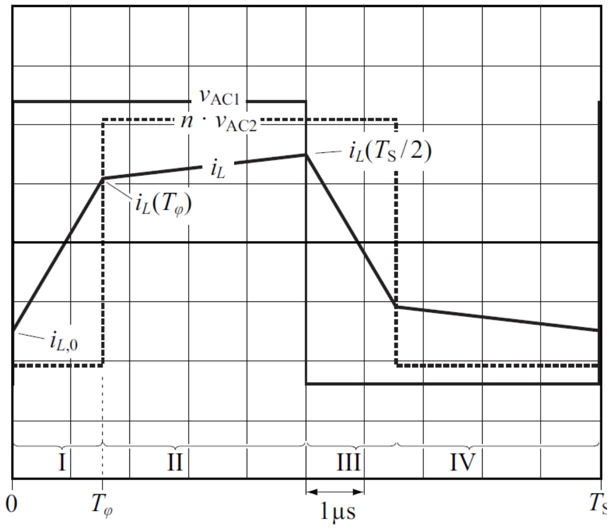

Figure 3. DAB current waveform under SPM method

C. Control principle of IPOS DAB

The advantage of Input Parallel Output Serial (IPOS) cascaded DAB converter structure is analyzed. The stability analysis of the simple IPOS DAB converter composed of two modules is shown as Figure 4.

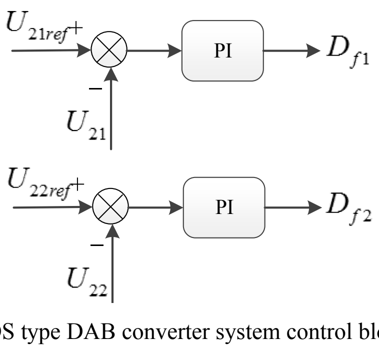

Figure 4. IPOS type DAB converter system control block diagram

Figure 5 is a controlled current source equivalent circuit model of an IPOS type DAB converter. Where:

$$g_{m1} = N_1 \frac{d_1(1-d_1)}{2fL_1} \tag{4}$$

$$g_{m2} = N_2 \frac{d_2(1-d_2)}{2fL_2} \tag{5}$$

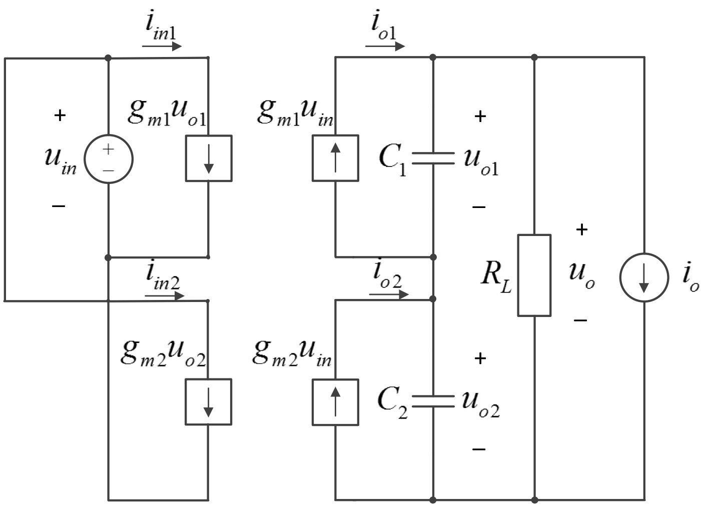

Figure 5. Controlled Current Source Equivalent Circuit Model of IPOS Type DAB Converter

Assume that in the ideal case the parameters of the two modules are the same, there is $N_1 = N_1 = N$, $L_1 = L_2 = L$, $C_1 = C_2 = C$, $D_1 = D_2 = D$.

Considering the small disturbances, the relationship between the disturbances can be obtained as follows:

$$\begin{cases} \hat{u}_o = \hat{u}_{o1} + \hat{u}_{o2} = \dfrac{R_L}{2+sCR_L}\left(\hat{i}_{o1} + \hat{i}_{o2} - 2\hat{i}_o\right) \\ \hat{u}_{o1} = \dfrac{1+sCR_L}{sC\left(2+sCR_L\right)}\hat{i}_{o1} - \dfrac{1}{sC\left(2+sCR_L\right)}\hat{i}_{o2} - \dfrac{R_L}{2+sCR_L}\hat{i}_o \\ \hat{u}_{o2} = -\dfrac{1}{sC\left(2+sCR_L\right)}\hat{i}_{o1} + \dfrac{1+sCR_L}{sC\left(2+sCR_L\right)}\hat{i}_{o2} - \dfrac{R_L}{2+sCR_L}\hat{i}_o \end{cases} \tag{6}$$

The model of control is as follows, where G_{od} is the transfer function of the PI controller.

$$\begin{cases} \hat{d}_1 = G_{od}\left(\hat{u}_{1ref} - \hat{u}_{o1}\right) \\ \hat{d}_2 = G_{od}\left(\hat{u}_{2ref} - \hat{u}_{o2}\right) \end{cases} \tag{7}$$

Assuming $\dfrac{U_{in}N\left(1-2D\right)}{2fL}G_{od} = k_p + \dfrac{k_i}{s}$, the denominator polynomial of the system transfer function can be obtained as:

$$P(s) = \left[s^2CR_L + \left(2+k_p\right)s + k_i\right]\left(sCR_L + 2\right) \tag{8}$$

It can be seen that through the reasonable PI regulator parameter design, the poles of the system can be controlled in the left half plane.

III. . Simulation and analysis

A simulation model of high voltage power supply was built in Matlab/Simulink based on the analysis as above. The input voltage is 100V, and the output voltage is 400V. It can be seen from the simulation waveform that the output voltage of a single module is finally stabilized at around 400V in 0.02s. The output voltage of IPOS system basing on the generic high voltage power supply module reaches the set point of 1200V as expected. The ripple is less than 5%. There is no oscillation when the output voltage reaches the referenced value.

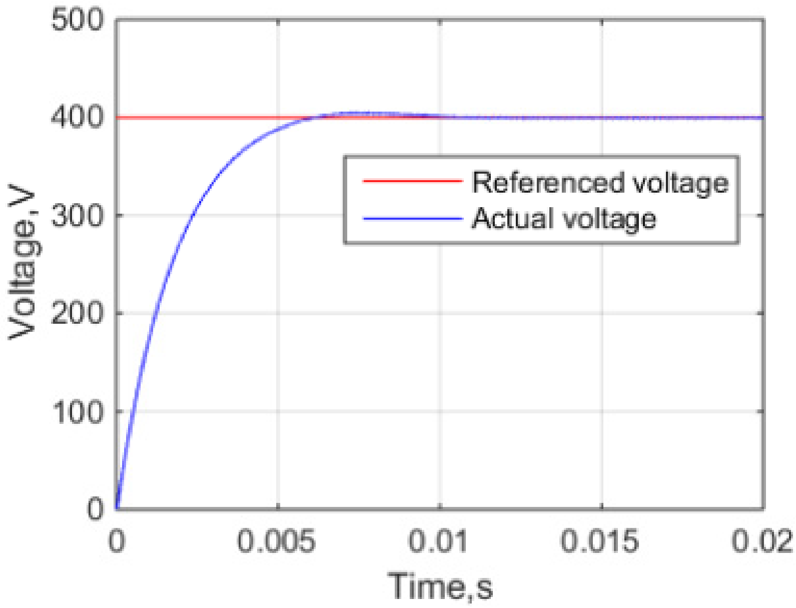

Figure 6. Voltage waveform for HVPS module

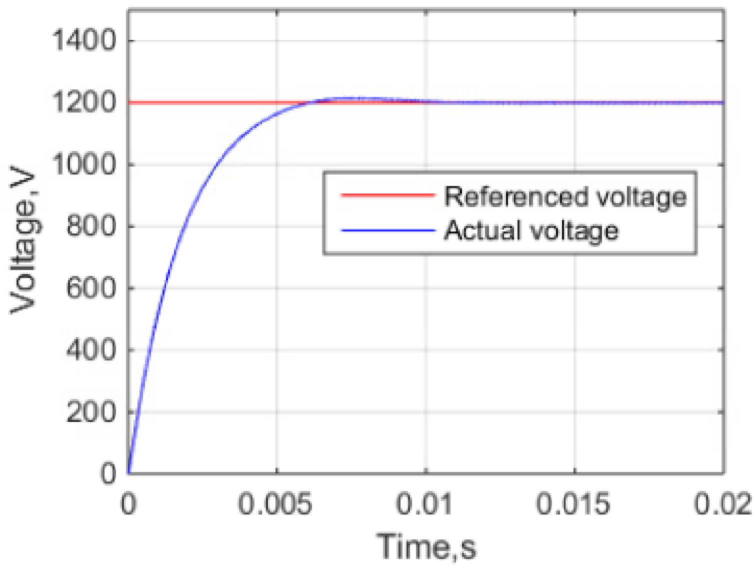

Figure 7. Voltage waveform for HVPS system

IV. Conclusion

DAB converter topology is applied to the satellite electric propulsion power supply. The topology comparison shows that the cascaded DAB converter is an optimal topology for the design, which makes the system high voltage, large capacity, high power density, high efficiency requirements are met. The high-frequency transformer is used to isolate the secondary side of each system from each other, and the cascading structure makes the system have the capability of fault-tolerant operation, which greatly improves the system reliability.

References

[1] Fernando PINTÓ, Javier PALENCIA, Nicoletta WAGNER, etc. “Power Processing Unit Activities in Airbus DS Space Equipments,” Proceedings of European Space Power Conference, Thessaloniki, Greece, 2016

[2]Thompson, C. M., “Spacecraft Thermal Control, Design, and Operation,” *Proceedings of European Space Power Conference*, Thessaloniki, Greece, 2016, pp. 1-6.

[3]Christian R._, Uwe P. ,Jens S., et cl. “Development of a controlled High Voltage Power Supply for Gridded Ion Thrusters”, *Proceedings of 35th International Electric Propulsion Conference* , Atlanta, USA, 2017, pp. 1-8

[4]Eric B., Stéphane F. “PPU MK3 for 5 KW hall effect thrusters ”, *Proceedings of European Space Power Conference*, Thessaloniki, Greece, 2016

[5]Matthias G., Michael B., Frank H., Bernhard K . “Generic High Voltage Power Supplies (HVPS) with Optimum Efficiency and Multi-Range”, *Proceedings of 30th International Electric Propulsion Conference, Florence, Italy 2007*

[6] J. Palencia. Electronics for Electric Propulsion Gridded Ion Technology, 2017

[7]Li Feng, Kang Qing , Xing Jie, et cl. “Technology for power processing unit used in high power electric propulsion”, Journal of Beijing University of Aeronautics and Astronautics, Vol.42, No.8, 21 Jan.2016, pp.1575-1583.

[8] Philippe F., Marc F., Paul M. & Michaël N. “GaN Transistor in Space Equipments: From Selection to applications”, *Proceedings of European Space Power Conference Thessaloniki, Greece, 2016*